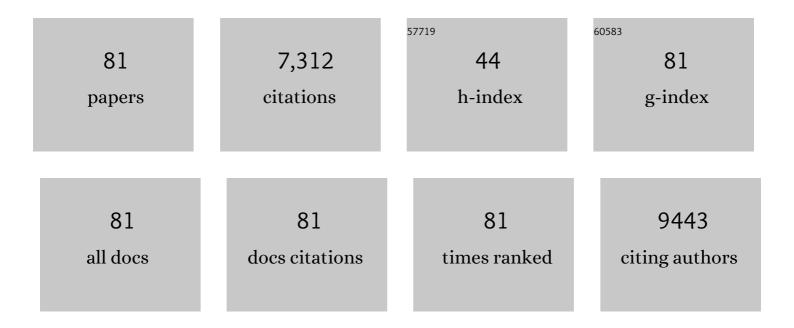
List of Publications by Year in descending order

Source: https://exaly.com/author-pdf/151902/publications.pdf Version: 2024-02-01



Ειιμινι Μιλο

#	Article	IF	CITATIONS
1	Electrospun Nanofibers of <i>p</i> -Type NiO/ <i>n</i> -Type ZnO Heterojunctions with Enhanced Photocatalytic Activity. ACS Applied Materials & Interfaces, 2010, 2, 2915-2923.	4.0	574
2	In situ assembly of well-dispersed Ag nanoparticles (AgNPs) on electrospun carbon nanofibers (CNFs) for catalytic reduction of 4-nitrophenol. Nanoscale, 2011, 3, 3357.	2.8	566
3	High Photocatalytic Activity of ZnOâ^'Carbon Nanofiber Heteroarchitectures. ACS Applied Materials & Interfaces, 2011, 3, 590-596.	4.0	415
4	Electrospun Nanofibers of ZnOâ^'SnO ₂ Heterojunction with High Photocatalytic Activity. Journal of Physical Chemistry C, 2010, 114, 7920-7925.	1.5	345
5	Highly dispersed Fe3O4 nanosheets on one-dimensional carbon nanofibers: Synthesis, formation mechanism, and electrochemical performance as supercapacitor electrode materials. Nanoscale, 2011, 3, 5034.	2.8	299
6	A Facile in Situ Hydrothermal Method to SrTiO ₃ /TiO ₂ Nanofiber Heterostructures with High Photocatalytic Activity. Langmuir, 2011, 27, 2946-2952.	1.6	269
7	Tubular nanocomposite catalysts based on size-controlled and highly dispersed silver nanoparticles assembled on electrospun silicananotubes for catalytic reduction of 4-nitrophenol. Journal of Materials Chemistry, 2012, 22, 1387-1395.	6.7	251
8	One-dimensional Bi2MoO6/TiO2 hierarchical heterostructures with enhanced photocatalytic activity. CrystEngComm, 2012, 14, 605-612.	1.3	228
9	Fabrication of Ag/TiO2 nanoheterostructures with visible light photocatalytic function via a solvothermal approach. CrystEngComm, 2012, 14, 3989.	1.3	225
10	Flexible solid-state supercapacitors based on freestanding nitrogen-doped porous carbon nanofibers derived from electrospun polyacrylonitrile@polyaniline nanofibers. Journal of Materials Chemistry A, 2016, 4, 4180-4187.	5.2	203
11	Hierarchical heterostructures of Bi2MoO6 on carbon nanofibers: controllable solvothermal fabrication and enhanced visible photocatalytic properties. Journal of Materials Chemistry, 2012, 22, 577-584.	6.7	196
12	<i>p</i> -MoO ₃ Nanostructures/ <i>n</i> -TiO ₂ Nanofiber Heterojunctions: Controlled Fabrication and Enhanced Photocatalytic Properties. ACS Applied Materials & Interfaces, 2014, 6, 9004-9012.	4.0	148
13	Core/shell nanofibers of TiO2@carbon embedded by Ag nanoparticles with enhanced visible photocatalytic activity. Journal of Materials Chemistry, 2011, 21, 17746.	6.7	143
14	Bi2MoO6 microtubes: Controlled fabrication by using electrospun polyacrylonitrile microfibers as template and their enhanced visible light photocatalytic activity. Journal of Hazardous Materials, 2012, 225-226, 155-163.	6.5	130
15	Polyaniline-coated electrospun carbon nanofibers with high mass loading and enhanced capacitive performance as freestanding electrodes for flexible solid-state supercapacitors. Energy, 2016, 95, 233-241.	4.5	122
16	Polyacrylonitrile and Carbon Nanofibers with Controllable Nanoporous Structures by Electrospinning. Macromolecular Materials and Engineering, 2009, 294, 673-678.	1.7	119
17	Three dimensional hierarchical heterostructures of g-C3N4 nanosheets/TiO2 nanofibers: Controllable growth via gas-solid reaction and enhanced photocatalytic activity under visible light. Journal of Hazardous Materials, 2018, 344, 113-122.	6.5	116
18	Bi4Ti3O12 nanosheets/TiO2 submicron fibers heterostructures: in situ fabrication and high visible light photocatalytic activity. Journal of Materials Chemistry, 2011, 21, 6922.	6.7	113

#	Article	IF	CITATIONS
19	In situ assembly of well-dispersed Au nanoparticles on TiO2/ZnO nanofibers: A three-way synergistic heterostructure with enhanced photocatalytic activity. Journal of Hazardous Materials, 2012, 237-238, 331-338.	6.5	113
20	Hydrothermal synthesis of carbon-rich graphitic carbon nitride nanosheets for photoredox catalysis. Journal of Materials Chemistry A, 2015, 3, 3281-3284.	5.2	113
21	One-dimensional hierarchical heterostructures of In2S3 nanosheets on electrospun TiO2 nanofibers with enhanced visible photocatalytic activity. Journal of Hazardous Materials, 2013, 260, 892-900.	6.5	103
22	Bi2MoO6/BiFeO3 heterojunction nanofibers: Enhanced photocatalytic activity, charge separation mechanism and magnetic separability. Journal of Colloid and Interface Science, 2018, 529, 404-414.	5.0	99
23	Three-dimensional freestanding hierarchically porous carbon materials as binder-free electrodes for supercapacitors: high capacitive property and long-term cycling stability. Journal of Materials Chemistry A, 2016, 4, 5623-5631.	5.2	89
24	Tin oxide (SnO2) nanoparticles/electrospun carbon nanofibers (CNFs) heterostructures: Controlled fabrication and high capacitive behavior. Journal of Colloid and Interface Science, 2011, 356, 706-712.	5.0	88
25	TiO ₂ /SrTiO ₃ /g-C ₃ N ₄ ternary heterojunction nanofibers: gradient energy band, cascade charge transfer, enhanced photocatalytic hydrogen evolution, and nitrogen fixation. Nanoscale, 2020, 12, 8320-8329.	2.8	88
26	Electrospinning of magnetical bismuth ferrite nanofibers with photocatalytic activity. Ceramics International, 2013, 39, 3511-3518.	2.3	83
27	Composition-controllable p-CuO/n-ZnO hollow nanofibers for high-performance H2S detection. Sensors and Actuators B: Chemical, 2019, 285, 495-503.	4.0	82
28	CuO/Cu ₂ O nanofibers as electrode materials for non-enzymatic glucose sensors with improved sensitivity. RSC Advances, 2014, 4, 31056.	1.7	79
29	Construction of In2O3/ZnO yolk-shell nanofibers for room-temperature NO2 detection under UV illumination. Journal of Hazardous Materials, 2021, 403, 124093.	6.5	75
30	ln ₂ O ₃ nanocubes/carbon nanofibers heterostructures with high visible light photocatalytic activity. Journal of Materials Chemistry, 2012, 22, 1786-1793.	6.7	72
31	Direct Z-scheme heterostructure of p-CuAl2O4/n-Bi2WO6 composite nanofibers for efficient overall water splitting and photodegradation. Journal of Colloid and Interface Science, 2019, 550, 170-179.	5.0	71
32	BiOCl nanosheets immobilized on electrospun polyacrylonitrile nanofibers with high photocatalytic activity and reusable property. Applied Surface Science, 2013, 285, 509-516.	3.1	70
33	Hierarchical heterostructures of p-type BiOCl nanosheets on electrospun n-type TiO2 nanofibers with enhanced photocatalytic activity. Catalysis Communications, 2015, 67, 6-10.	1.6	70
34	3D MoS 2 nanosheet/TiO 2 nanofiber heterostructures with enhanced photocatalytic activity under UV irradiation. Journal of Alloys and Compounds, 2016, 686, 137-144.	2.8	69
35	Hollow CuFe2O4/α-Fe2O3 composite with ultrathin porous shell for acetone detection at ppb levels. Sensors and Actuators B: Chemical, 2018, 258, 436-446.	4.0	61
36	Discrete heterojunction nanofibers of BiFeO3/Bi2WO6: Novel architecture for effective charge separation and enhanced photocatalytic performance. Journal of Colloid and Interface Science, 2020, 572, 257-268.	5.0	60

#	Article	IF	CITATIONS
37	Sn-doping induced oxygen vacancies on the surface of the In2O3 nanofibers and their promoting effect on sensitive NO2 detection at low temperature. Sensors and Actuators B: Chemical, 2020, 317, 128194.	4.0	60
38	Assembling n-Bi ₂ MoO ₆ Nanosheets on Electrospun p-CuAl ₂ O ₄ Hollow Nanofibers: Enhanced Photocatalytic Activity Based on Highly Efficient Charge Separation and Transfer. ACS Sustainable Chemistry and Engineering, 2018, 6, 10714-10723.	3.2	59
39	Reusable and Flexible g-C ₃ N ₄ /Ag ₃ PO ₄ /Polyacrylonitrile Heterojunction Nanofibers for Photocatalytic Dye Degradation and Oxygen Evolution. ACS Applied Nano Materials, 2019. 2. 3081-3090.	2.4	58
40	Dandelion-like Fe3O4@CuTNPc hierarchical nanostructures as a magnetically separable visible-light photocatalyst. Journal of Materials Chemistry, 2011, 21, 12083.	6.7	54
41	Magnetically separable Bi2MoO6/ZnFe2O4 heterostructure nanofibers: Controllable synthesis and enhanced visible light photocatalytic activity. Journal of Alloys and Compounds, 2018, 747, 916-925.	2.8	50
42	Flexible solid-state supercapacitors based on freestanding electrodes of electrospun polyacrylonitrile@polyaniline core-shell nanofibers. Electrochimica Acta, 2015, 176, 293-300.	2.6	46
43	Octahedral-Like CuO/In ₂ O ₃ Mesocages with Double-Shell Architectures: Rational Preparation and Application in Hydrogen Sulfide Detection. ACS Applied Materials & Interfaces, 2017, 9, 44632-44640.	4.0	46
44	Graphitic carbon nitride/BiOI loaded on electrospun silica nanofibers with enhanced photocatalytic activity. Applied Surface Science, 2018, 455, 952-962.	3.1	46
45	TiO2 nanoparticles immobilized on polyacrylonitrile nanofibers mats: a flexible and recyclable photocatalyst for phenol degradation. RSC Advances, 2013, 3, 7503.	1.7	44
46	Freestanding hierarchically porous carbon framework decorated by polyaniline as binder-free electrodes for high performance supercapacitors. Journal of Power Sources, 2016, 329, 516-524.	4.0	44
47	In2S3/carbon nanofibers/Au ternary synergetic system: Hierarchical assembly and enhanced visible-light photocatalytic activity. Journal of Hazardous Materials, 2015, 283, 599-607.	6.5	43
48	Controllable fabrication of cadmium phthalocyanine nanostructures immobilized on electrospun polyacrylonitrile nanofibers with high photocatalytic properties under visible light. Catalysis Communications, 2011, 12, 880-885.	1.6	42
49	Hierarchical heterostructures of p-type bismuth oxychloride nanosheets on n-type zinc ferrite electrospun nanofibers with enhanced visible-light photocatalytic activities and magnetic separation properties. Journal of Colloid and Interface Science, 2018, 516, 110-120.	5.0	42
50	Highly electron-depleted ZnO/ZnFe2O4/Au hollow meshes as an advanced material for gas sensing application. Sensors and Actuators B: Chemical, 2019, 297, 126769.	4.0	42
51	Bismuth oxychloride (BiOCl)/copper phthalocyanine (CuTNPc) heterostructures immobilized on electrospun polyacrylonitrile nanofibers with enhanced activity for floating photocatalysis. Journal of Colloid and Interface Science, 2018, 525, 187-195.	5.0	40
52	ZnO/ZnFe ₂ O ₄ Janus Hollow Nanofibers with Magnetic Separability for Photocatalytic Degradation of Water-Soluble Organic Dyes. ACS Applied Nano Materials, 2019, 2, 4879-4890.	2.4	38
53	Nitrogen doping polyvinylpyrrolidone-based carbon nanofibers via pyrolysis of g-C3N4 with tunable chemical states and capacitive energy storage. Electrochimica Acta, 2020, 330, 135212.	2.6	38
54	Heterojunctions of p-BiOI Nanosheets/n-TiO2 Nanofibers: Preparation and Enhanced Visible-Light Photocatalytic Activity. Materials, 2016, 9, 90.	1.3	35

#	Article	IF	CITATIONS
55	Immobilization of ZnO/polyaniline heterojunction on electrospun polyacrylonitrile nanofibers and enhanced photocatalytic activity. Materials Chemistry and Physics, 2018, 214, 507-515.	2.0	35
56	MoSe ₂ /TiO ₂ Nanofibers for Cycling Photocatalytic Removing Water Pollutants under UV–Vis–NIR Light. ACS Applied Nano Materials, 2020, 3, 2278-2287.	2.4	35
57	Bi2WO6/ZnFe2O4 heterostructures nanofibers: Enhanced visible-light photocatalytic activity and magnetically separable property. Materials Research Bulletin, 2018, 104, 124-133.	2.7	34
58	Fabrication of g-C3N4/SiO2-Au composite nanofibers with enhanced visible photocatalytic activity. Ceramics International, 2017, 43, 15699-15707.	2.3	34
59	Solvothermal synthesis and electrochemical properties of 3D flower-like iron phthalocyanine hierarchical nanostructure. Nanoscale, 2011, 3, 5126.	2.8	30
60	A self-floating electrospun nanofiber mat for continuously high-efficiency solar desalination. Chemosphere, 2021, 280, 130719.	4.2	29
61	Three-dimensional hierarchical CeO2 nanowalls/TiO2 nanofibers heterostructure and its high photocatalytic performance. Journal of Sol-Gel Science and Technology, 2010, 55, 105-110.	1.1	28
62	Molybdenum diselenide nanosheet/carbon nanofiber heterojunctions: Controllable fabrication and enhanced photocatalytic properties with a broad-spectrum response from visible to infrared light. Journal of Colloid and Interface Science, 2018, 518, 1-10.	5.0	28
63	Three-dimensional porous CuFe2O4 for visible-light-driven peroxymonosulfate activation with superior performance for the degradation of tetracycline hydrochloride. Chemical Engineering Journal, 2022, 445, 136616.	6.6	27
64	Highly permeable WO3/CuWO4 heterostructure with 3D hierarchical porous structure for high-sensitive room-temperature visible-light driven gas sensor. Sensors and Actuators B: Chemical, 2022, 365, 131926.	4.0	26
65	Hierarchically Porous In2O3/In2S3 Heterostructures as Micronano Photocatalytic Reactors Prepared by a Novel Polymer-Assisted Sol–Gel Freeze-Drying Method. Industrial & Engineering Chemistry Research, 2019, 58, 14106-14114.	1.8	25
66	Integrated structural design of polyaniline-modified nitrogen-doped hierarchical porous carbon nanofibers as binder-free electrodes toward all-solid-state flexible supercapacitors. Applied Surface Science, 2020, 501, 144001.	3.1	25
67	Flexible Allâ€Inorganic Roomâ€Temperature Chemiresistors Based on Fibrous Ceramic Substrate and Visibleâ€Lightâ€Powered Semiconductor Sensing Layer. Advanced Science, 2021, 8, e2102471.	5.6	21
68	Bismuth oxychloride/carbon nanofiber heterostructures for the degradation of 4-nitrophenol. CrystEngComm, 2015, 17, 7276-7282.	1.3	20
69	Immobilization of ultrafine Ag nanoparticles on well-designed hierarchically porous silica for high-performance catalysis. Journal of Colloid and Interface Science, 2018, 530, 345-352.	5.0	19
70	Electrospun CuAl ₂ O ₄ hollow nanofibers as visible light photocatalyst with enhanced activity and excellent stability under acid and alkali conditions. CrystEngComm, 2018, 20, 312-322.	1.3	18
71	Enhanced Full-Spectrum-Response Photocatalysis and Reusability of MoSe ₂ via Hierarchical N-Doped Carbon Nanofibers as Heterostructural Supports. ACS Sustainable Chemistry and Engineering, 2018, 6, 14314-14322.	3.2	16
72	One-dimensional heterostructures of beta-nickel hydroxide nanoplates/electrospun carbon nanofibers: Controlled fabrication and high capacitive property. International Journal of Hydrogen Energy, 2014, 39, 16162-16170.	3.8	14

#	Article	IF	CITATIONS
73	Anchoring bismuth oxybromo-iodide solid solutions on flexible electrospun polyacrylonitrile nanofiber mats for floating photocatalysis. Journal of Colloid and Interface Science, 2022, 608, 3178-3191.	5.0	13
74	Controllable synthesis and enhanced visible photocatalytic degradation performances of Bi2WO6–carbon nanofibers heteroarchitectures. Journal of Sol-Gel Science and Technology, 2014, 70, 149-158.	1.1	12
75	Room temperature immobilized BiOI nanosheets on flexible electrospun polyacrylonitrile nanofibers with high visible-light photocatalytic activity. Journal of Sol-Gel Science and Technology, 2016, 80, 783-792.	1.1	12
76	Facile preparation of flexible polyacrylonitrile/BiOCl/BiOI nanofibers via SILAR method for effective floating photocatalysis. Journal of Sol-Gel Science and Technology, 2021, 97, 610-621.	1.1	12
77	A Poreâ€Forming Strategy Toward Porous Carbonâ€Based Substrates for High Performance Flexible Lithium Metal Full Batteries. Energy and Environmental Materials, 2023, 6, .	7.3	8
78	Oxidation of phthalate acid esters using hydrogen peroxide and polyoxometalate/graphene hybrids. Journal of Hazardous Materials, 2022, 422, 126867.	6.5	7
79	Combination effects of ellagic acid with erlotinib in a Ba/ F3 cell line expressing EGFR H773_V774 insH mutation. Thoracic Cancer, 2020, 11, 2101-2111.	0.8	5
80	Controllable preparation of three-dimensional porous WO3 with enhanced visible light photocatalytic activity via a freeze-drying method. Journal of Materials Science: Materials in Electronics, 2018, 29, 9605-9612.	1.1	4
81	<scp>Heteroâ€Janus</scp> Nanofibers as an Ideal Framework for Promoting Waterâ€pollutant Photoreforming Hydrogen Evolution. Energy and Environmental Materials, 2023, 6, .	7.3	1